



ELSEVIER

Journal of Alloys and Compounds 218 (1995) 110–116

Journal of
ALLOYS
AND COMPOUNDS

The magnetic properties of BaLaCoIrO_6 and $\text{Ba}_3\text{CoIr}_x\text{Ru}_{2-x}\text{O}_9$

P.D. Battle ^{*,a}, J.G. Gore ^a, R.C. Hollyman ^a, A.V. Powell ^b^a *Inorganic Chemistry Laboratory, South Parks Road, Oxford OX1 3QR, UK*^b *Chemistry Department, Heriot-Watt University, Riccarton, Edinburgh EH14 4AS, UK*

Received 24 June 1994; in final form 17 August 1994

Abstract

The magnetic structure of the antiferromagnetic phase of the pseudo-cubic perovskite BaLaCoIrO_6 has been determined from time-of-flight powder neutron diffraction data collected at a temperature of 4 K. The Co(II) cations adopt a Type II collinear spin structure with an ordered moment of $2.8(2) \mu_B$ per Co(II); the Ir(V) cations do not have a detectable ordered magnetic moment. Magnetic susceptibility measurements on the compounds $\text{Ba}_3\text{CoIr}_x\text{Ru}_{2-x}\text{O}_9$ ($0 < x \leq 2$) resulted in the observation of weak ferromagnetism; the saturation magnetization decreased with increasing Ru content. Comparisons are made between BaLaCoIrO_6 and the spin glass BaLaCoRuO_6 , and also between $\text{Ba}_3\text{CoIr}_2\text{O}_9$ and antiferromagnetic $\text{Ba}_3\text{CoRu}_2\text{O}_9$. The behaviour of the nominally non-magnetic Ir(V) cations is discussed and contrasted with that of diamagnetic Sb(V) in $\text{Ba}_3\text{CoSb}_2\text{O}_9$ and $\text{Ba}_3\text{CoIrSbO}_9$.

Keywords: Magnetic structure; Antiferromagnetic phase; Neutron diffraction

1. Introduction

Recently, mixed metal oxides containing iridium have been the focus for a lot of research activity. Interest has centred on their structural chemistry [1], their defect chemistry [2], and their electronic properties [3]. Most of the work has been concerned with the oxidation state Ir(IV), although Ir(V) [4,5] and Ir(VI) [6] have also been studied. Ir(V) is a relatively unusual oxidation state in mixed metal oxides, and has previously attracted limited interest because the $5d^4$ electron configuration leads to a non-magnetic ($j=0$) ground state when the cation occupies a site of cubic symmetry. Our own research has been primarily concerned with compounds containing the magnetic cation Ru(V), which is comparable in size to Ir(V) and therefore shows a similar structural chemistry. We have previously [7] shown that BaLaCoRuO_6 has a pseudo-cubic, perovskite-like crystal structure with a disordered arrangement of Ba and La over the larger cation sites and a partially ($\approx 10\%$) ordered Co/Ru distribution over the octahedral sites; the compound shows a transition to a spin glass state at 40 K. This magnetic behaviour contrasts with that found in the hexagonal 6H perovskite $\text{Ba}_3\text{CoRu}_2\text{O}_9$, which is antiferromagnetic below 106 K; in this compound the Co and Ru cations occupy the vertex-sharing

and face-sharing octahedral sites in a fully ordered fashion [8]. We have now begun to investigate the consequences for these materials of replacing Ru with Ir, and we describe below the results of magnetic susceptibility measurements on the solid solution $\text{Ba}_3\text{CoIr}_x\text{Ru}_{2-x}\text{O}_9$, and a low-temperature neutron diffraction study of BaLaCoIrO_6 ; the room temperature crystal structure and the magnetic susceptibility of the latter compound have already been reported [3].

2. Experimental

The preparation of a polycrystalline sample of BaLaCoIrO_6 has been described previously [3]. Compositions in the series $\text{Ba}_3\text{CoIr}_x\text{Ru}_{2-x}\text{O}_9$ were prepared by firing pelletized mixtures of the appropriate stoichiometric quantities of dry BaCO_3 , La_2O_3 , Co_3O_4 , RuO_2 and Ir metal (all Johnson Matthey Chemicals) in alumina crucibles. All firings were carried out in air, initially at 500 °C and subsequently at 950 °C, for a period of several days. Samples of $\text{Ba}_3\text{CoSb}_2\text{O}_9$ and $\text{Ba}_3\text{CoIrSbO}_9$ were prepared for reference purposes by firing stoichiometric mixtures of Co_3O_4 , Sb_2O_3 , Ir and BaCO_3 at up to 950 °C in the case of the former and at up to 1250 °C in the case of the latter. The progress of the syntheses was monitored using a Philips PW1710 X-ray powder diffractometer operating with CuK_α ra-

* Corresponding author.

diation in Bragg–Brentano geometry. The reactions were considered to be complete when further heating produced no change in the diffraction pattern. A diffraction pattern of the final product was collected over the angular range $5 < 2\theta < 100^\circ$ using a 2θ step size of 0.02° ; these data were analysed using the GSAS program package [9]. Magnetic susceptibility measurements were made in the temperature range $6 < T < 296$ K using a CCL SCU500 SQUID magnetometer. Data were collected after cooling the sample in the absence of an applied magnetic field (ZFC) and after cooling in the measuring field (FC) of 0.1 T (0.01 T in the case of the strongly magnetic sample $\text{Ba}_3\text{CoIr}_2\text{O}_9$). Time-of-flight neutron diffraction data were collected on a weighed (ca. 5 g) sample of BaLaCoIrO_6 , contained in a vanadium can at a temperature of 4 K, using the diffractometer POLARIS at the ISIS neutron source. The instrument was operating in its high-intensity, medium resolution mode. Profile analysis of the data was carried out using the GSAS program package [9].

3. Results

3.1. The magnetic structure of BaLaCoIrO_6

Two of the detector banks available on the POLARIS diffractometer were used in the analysis of the low-temperature phase of BaLaCoIrO_6 ; the A-bank at $2\theta = 20^\circ$, which covers relatively high d -spacings at a relatively low resolution, and the C-bank at $2\theta = 145^\circ$, which covers lower d -spacings at a higher resolution. The data from both banks were summed, normalized, and corrected for the significant absorption caused by the presence of iridium in the sample [10]. The following scattering lengths were used in all structure refinements: $b_{\text{Ba}} = 0.525$, $b_{\text{La}} = 0.827$, $b_{\text{Co}} = 0.253$, $b_{\text{Ir}} = 1.06$ and $b_{\text{O}} = 0.5805 \times 10^{-14}$ m. More Bragg peaks were visible, particularly at high d -spacing, in the data collected at 4 K than had been apparent at room temperature [3], and we assumed that this additional scattering was due to the presence of long-range magnetic order at low temperatures. Initially the room temperature structure was taken as the starting point for a refinement of the 4 K crystal structure using the low d -spacing (0.6–3.1 Å) C-bank data, with the magnetic Bragg peaks excluded. The magnetic structure was then refined using the A-bank data (1.0–6.5 Å) with the crystal structure held in the previously determined form. This strategy resulted in a final agreement factor (R_{wpr}) of 2.4% for the C-bank data and $R_{\text{wpr}} = 3.5\%$ for the A-bank data. Six unit cell parameters, twelve background terms, six peak-shape parameters, a scale factor, twelve atomic parameters and the intensities of 970 Bragg peaks were involved in the analysis of the C-bank data. The overall isotropic temperature factor had to be held constant

at zero to avoid physically meaningless values; this is probably an indication of a slight inadequacy in the absorption correction. Only the background parameters, the scale factor and the components of the ordered magnetic moment were varied during the analysis of the A-bank data, the instrumental parameters being held at values determined in a refinement of the room temperature structure from A-bank data. The need to use this convoluted structure refinement sequence is a consequence of using a diffractometer on a pulsed neutron source which is not optimized for magnetic diffraction, rather than a constant wavelength source which is suitable for both structural and magnetic studies.

The crystal structure at 4 K is essentially unchanged from that found at room temperature [3]. It can be described as a pseudo-cubic perovskite with a 1:1 alternate ordering of Co and Ir over the six-coordinate sites and a disordered arrangement of Ba and La over the larger cation sites. The symmetry is actually lowered as far as triclinic by the small distortions present, and the 4 K unit cell parameters refined to the following values: $a = 5.6270(5)$, $b = 5.6762(5)$, $c = 7.9589(7)$ Å, $\alpha = 89.98(1)$, $\beta = 89.92(1)$, $\gamma = 90.04(1)^\circ$. This choice of unit cell facilitates comparisons with other perovskites, but requires the use of the non-standard space group $\bar{1}$. The refined atomic coordinates are listed in Table 1. The high degree of pseudo-symmetry in the structure leads to relatively high standard deviations in the atomic coordinates and hence in the bond lengths. The Ir–O distances range from 1.986(9) to 1.992(7) Å and the Co–O distances from 2.012(9) to 2.071(7) Å. The observed distribution of magnetic Bragg scattering was consistent with the adoption of a Type II antiferromagnetic structure with only one set of six-coordinate sites occupied by a magnetic cation (Fig. 1). The magnetic cations lie in ferromagnetic sheets, with antiferromagnetic coupling between neighbouring sheets; the sheets are parallel to the (101) plane in a doubled unit cell. In the light of our previous work [3], the magnetic cation was assumed to be Co^{2+} and the magnetic form factor measured by Khan and Erickson [11] was used to model the angular dependence of the magnetic scattering length. The ordered component of the magnetic moment was then refined to a value of

Table 1
Structural parameters of BaLaCoIrO_6 at 4 K (space group $\bar{1}$)

Atom	x	y	z
Ba/La	0.499(2)	0.499(1)	0.250(1)
Co	0	1/2	0
Ir	1/2	0	0
O(1)	0.232(1)	0.222(1)	−0.0396(6)
O(2)	0.255(2)	0.749(2)	0.0091(7)
O(3)	0.517(1)	0.0475(7)	0.247(1)

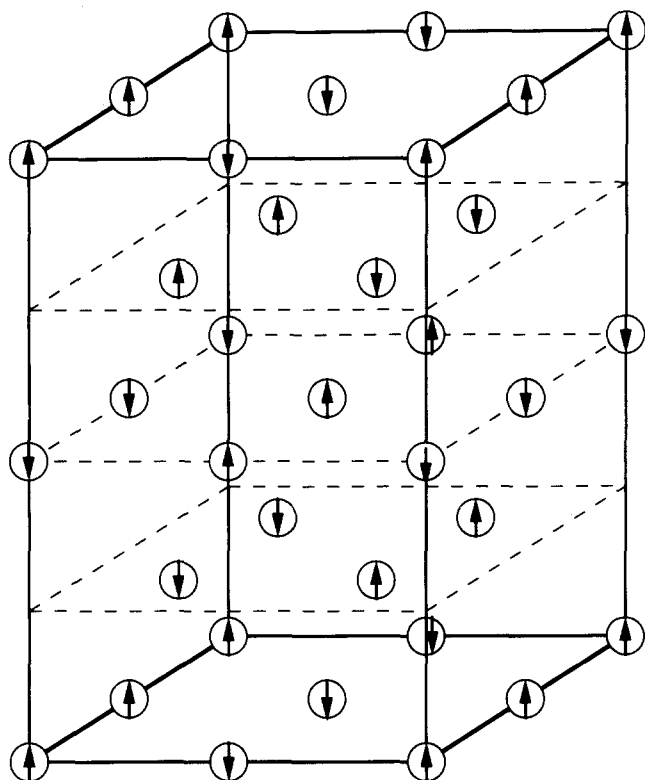
BaLaCoIrO₆

Fig. 1. The magnetic structure of BaLaCoIrO₆. Only the Co atoms are shown in the magnetic unit cell, which is derived from the crystallographic unit cell by a doubling along each axis.

2.8(2) μ_B , with components along the crystallographic axes of $m_x = 1.2(6)$, $m_y = 1.8(3)$ and $m_z = 1.7(5)$ μ_B . The standard deviations on these values indicate that our data define the magnitude of the magnetic moment more precisely than its orientation and, because of the complexity of the structure and the limitations of the POLARIS diffractometer, our study cannot be said to be of high resolution. The final observed, calculated and difference diffraction profiles from the A-bank are shown in Fig. 2; the change in background level at low d -spacing is due to scattering from the cryostat.

3.2. The crystal structure and magnetic properties of Ba₃CoIr_xRu_{2-x}O₉

Our attempts to prepare Ba₃CoIr_xRu_{2-x}O₉ with $x = 0.25, 0.5, 1.0, 1.5, 1.85$ and 2.0 resulted in black powders, the X-ray diffraction patterns of which could all be indexed in the hexagonal space group P6₃/mmc, with unit cell parameters (Table 2) characteristic of the 6H perovskite structure drawn in Fig. 3. Profile analysis of the X-ray data, performed using the GSAS package, confirmed the crystal structure assignment and suggested that in all cases the MO₆ octahedra, which

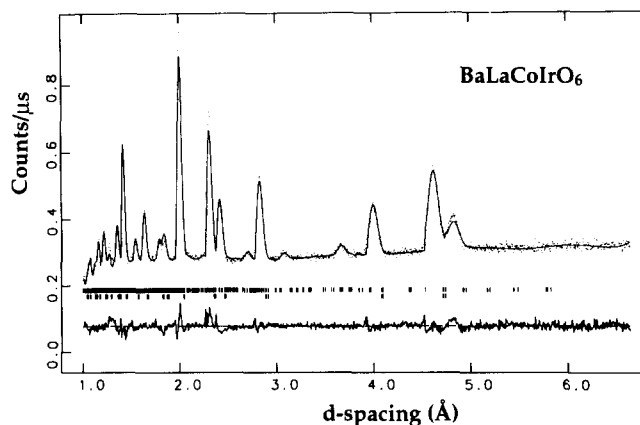


Fig. 2. The final observed, calculated and difference diffraction profiles from the refinement of the high d -spacing neutron diffraction data collected on BaLaCoIrO₆ at 4 K. The lower (upper) set of reflection markers refer to the crystallographic (magnetic) structure.

Table 2
Unit cell parameters for Ba₃CoIr_xRu_{2-x}O₉

x	a (Å)	c (Å)
0.25	5.7535(1)	14.1390(4)
0.50	5.7563(1)	14.1612(4)
1.00	5.7549(2)	14.1902(5)
1.50	5.7564(1)	14.2332(4)
1.85	5.7580(1)	14.2695(3)
2.00	5.7601(2)	14.2857(4)

are linked only through their vertices, are occupied by Co, and that the octahedra which share a face to form an M₂O₉ dimer are occupied by a disordered arrangement of Ir and Ru. However, the quality of our refinements (for example, $R_I = 7.8\%$, $R_{wpr} = 13.5\%$ for $x = 2$) was not sufficiently high to merit full publication of the structural parameters. The results of our magnetic susceptibility measurements are plotted in Fig. 4. The samples with $x = 2.0$ and 1.85 behave in a similar manner to each other and show magnetic phase transitions at ≈ 108 K; the hysteresis in the susceptibilities suggests that the low-temperature phase is a weak ferromagnet (a canted antiferromagnet), with the strength of the magnetization being a function of temperature in the range $40 < T < 100$ K. The samples with $x = 1.5, 1.0$, and 0.5 behave in a similar manner to each other and show magnetic phase transitions at 111 K, 108 K and ≈ 96 K respectively. The data suggest that the transition is to a canted magnetic structure in each case. The maximum value of the magnetic moment per formula unit is plotted as a function of composition in Fig. 5. The behaviour of the sample with an Ir content $x = 0.25$ differs markedly from that of the other compositions in that the FC and ZFC susceptibilities diverge at 208 K rather than at ≈ 100 K, although the ZFC data do show a maximum at 106 K. The interpretation of these observations will be discussed below.

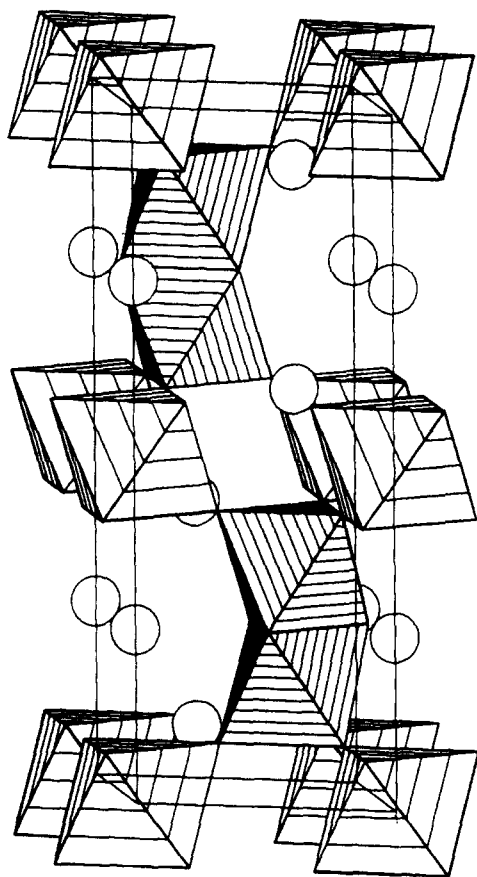


Fig. 3. The 6H perovskite structure of $\text{Ba}_3\text{CoIr}_2\text{O}_9$. Hollow circles represent Ba atoms, densely shaded octahedra Ir_2O_6 dimers and lightly shaded octahedra CoO_6 units.

3.3. The crystal structure and magnetic susceptibility of $\text{Ba}_3\text{CoSb}_2\text{O}_9$ and $\text{Ba}_3\text{CoIrSbO}_9$

The X-ray powder diffraction pattern of $\text{Ba}_3\text{CoSb}_2\text{O}_9$ was satisfactorily interpreted ($R_1 = 4.3\%$, $R_{\text{wpr}} = 11.6\%$) using profile analysis, whereas that of $\text{Ba}_3\text{CoIrSbO}_9$ was analysed in a slightly less convincing way ($R_1 = 4.6\%$, $R_{\text{wpr}} = 12.8\%$). However, it is clear that both compounds adopt a 6H perovskite structure (space group $\text{P6}_3/\text{mmc}$) with the vertex-sharing octahedra occupied by Co. The unit cell parameters of $\text{Ba}_3\text{CoSb}_2\text{O}_9$ refined to the values $a = 5.8533(1)$, $c = 14.4429(3)$ Å, in reasonable agreement with those reported previously [12], and those of $\text{Ba}_3\text{CoIrSbO}_9$, to $a = 5.8081(1)$, $c = 14.3732(4)$ Å. The mean Co–O and Sb–O bond lengths in the former refined to values of 2.02 Å and 2.09 Å respectively. The temperature dependence of the molar magnetic susceptibilities is plotted in Fig. 6; both the FC and ZFC values continue to increase down to the lowest temperatures, although a small hysteresis is apparent below 60 K ($\text{Ba}_3\text{CoSb}_2\text{O}_9$) or 72 K ($\text{Ba}_3\text{CoIrSbO}_9$). Fitting a Curie–Weiss Law in the temperature region $200 < T < 296$ K resulted in the values $m_{\text{eff}} = 5.6 \mu_{\text{B}}$, $\theta = -103.5$ K and $m_{\text{eff}} = 5.1$, $\theta = -53.8$ K respectively. It is notable that the molar susceptibilities of the two

compounds are essentially equal at room temperature, but that of the Ir-containing material increases more rapidly at low temperatures.

4. Discussion

We have previously reported [3] that the magnetic susceptibility of BaLaCoIrO_6 shows a maximum at 56 K, with no hysteresis apparent at lower temperatures. By considering the effective magnetic moment measured at higher temperatures and by comparing the behaviour of this compound with that of the Ni analogue, we were able to assign the cation oxidation states as Co(II) and Ir(V) rather than Co(III) and Ir(IV). This conclusion was consistent with the Co–O and Ir–O bond lengths determined in a room temperature neutron diffraction study [3]. The crystal and magnetic structures of the antiferromagnetic phase determined in the present study are also consistent with our assignment, with only the Co(II) cations showing an ordered magnetic moment. The distortion of the first coordination shell around the Ir(V) cations is slight enough for the symmetry to be treated as pseudo-cubic, in which case Ir(V) is expected to have an electronic ground state which is only weakly magnetic [4,5,13]. The ordered magnetic moment on the Co ions is comparable to the value of $2.71(5) \mu_{\text{B}}$ observed previously in $\text{Ba}_3\text{CoRu}_2\text{O}_9$, although the precision of the measurement is somewhat lower in the present case. This imprecision is due partly to the low neutron flux on POLARIS at the longer wavelengths needed in a magnetic diffraction experiment and partly to the low symmetry of the magnetic structure. The relatively low value of the magnetic moment suggests that there is a high degree of covalency in the bonding around the magnetic cations. The adoption of a Type II magnetic structure indicates that the pseudo-linear next-nearest-neighbour Co–O–Ir–O–Co superexchange interaction is stronger than that between nearest-neighbour Co atoms, even though the former occurs over a longer distance (≈ 8 Å) than the latter (≈ 5.65 Å). The reverse is true in many compounds, particularly those in which the cation e_g orbitals are empty and hence unable to create a strong σ superexchange interaction [14]. The magnetic properties of BaLaCoIrO_6 are thus very different from those of the structurally disordered spin glass BaLaCoRuO_6 . They are, however, consistent with those of other pseudo-cubic Ir(V) perovskites, for example BaLaMgIrO_6 [5].

It has been established previously [15] that $\text{Ba}_3\text{CoRu}_2\text{O}_9$ and $\text{Ba}_3\text{CoIr}_2\text{O}_9$ both adopt the 6H hexagonal perovskite structure, and our structural data show that the same structure is maintained throughout the system $\text{Ba}_3\text{CoIr}_x\text{Ru}_{2-x}\text{O}_9$. The unit cell parameters generally show a steady increase with Ir content, al-

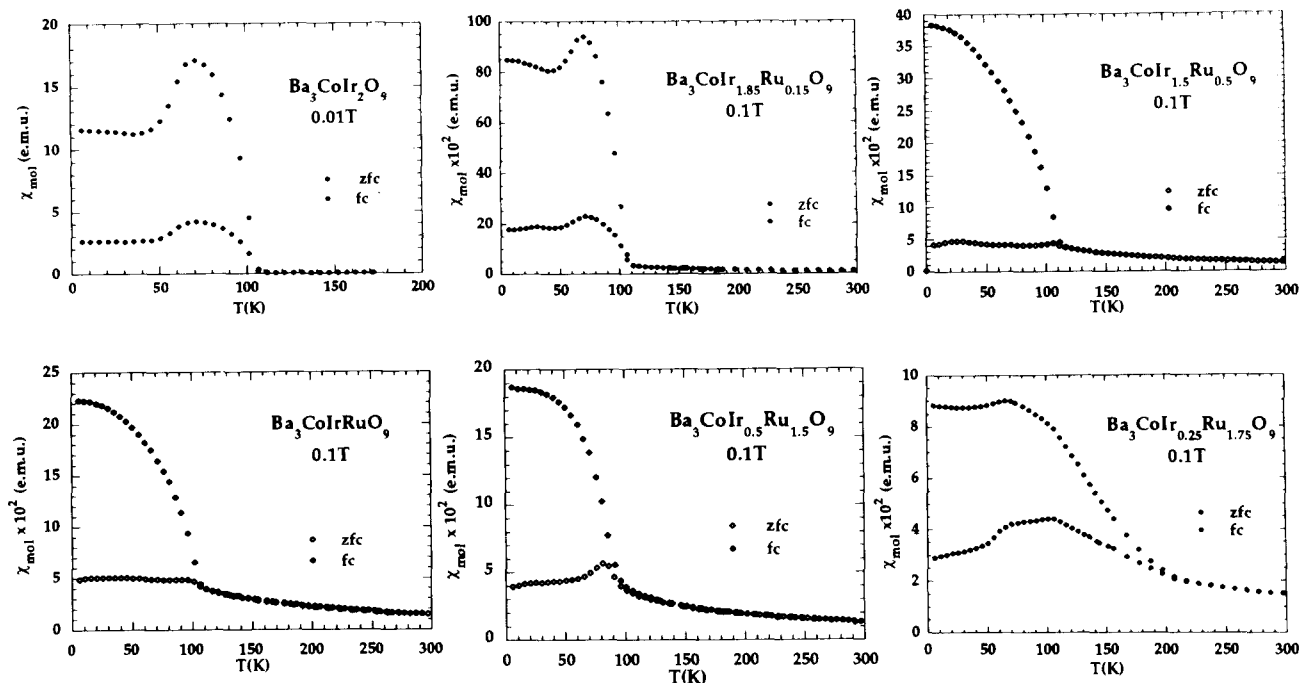


Fig. 4. The temperature dependence of the molar magnetic susceptibility of $\text{Ba}_3\text{CoIr}_x\text{Ru}_{2-x}\text{O}_9$.

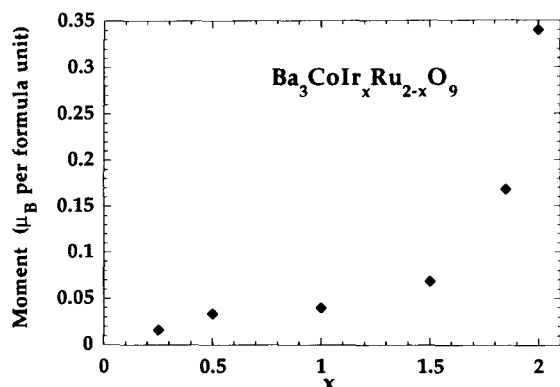


Fig. 5. The maximum magnetic moment per formula unit of $\text{Ba}_3\text{CoIr}_x\text{Ru}_{2-x}\text{O}_9$ as a function of Ir content.

though there is an unexplained anomaly in the value of the a parameter for the sample $x=0.5$. The magnetic behaviour of $\text{Ba}_3\text{CoIr}_2\text{O}_9$ is strikingly different from that of both $\text{Ba}_3\text{CoSb}_2\text{O}_9$ and antiferromagnetic $\text{Ba}_3\text{CoRu}_2\text{O}_9$ [7,8]. In the interpretation of the data on the latter compound it was assumed that the localized magnetic moments of the dimeric Ru cations couple antiferromagnetically at high (>300 K) temperatures, and that their interaction with the Co cations leads to the onset of long-range magnetic order at the Neel temperature of 106 K. The assumption concerning the behaviour of the spins within the dimers was based on a previous study of $\text{Ba}_3\text{CaRu}_2\text{O}_9$ [16]. The similarity of the magnetic ordering temperatures of $\text{Ba}_3\text{CoIr}_2\text{O}_9$ and $\text{Ba}_3\text{CoRu}_2\text{O}_9$ suggests that the transition observed at 108 K in the former is also due to the magnetic ordering of the Co sublattice, but leading in this case

to the formation of a weak ferromagnet rather than an antiferromagnet. It is implicit in this explanation that the superexchange involves spin-coupled Ir_2O_9 groups, just as the Ru_2O_9 dimers were involved in the analogous compound of Ru, and hence that the Ir cations have a significant magnetic moment in this compound, unlike in BaLaCoIrO_6 . Our data show that $\text{Ba}_3\text{CoSb}_2\text{O}_9$, a compound in which the dimers are occupied by diamagnetic cations, does not transform to a magnetically ordered state, and there is no evidence for short-range spin cluster formation above 60 K (the hysteresis observed below this temperature presumably stems from frustrated Co–O–O–Co interactions [8]). Nor was a magnetically ordered state found in $\text{Ba}_3\text{CoIrSbO}_9$, although the susceptibility of this compound does rise more rapidly than that of the Ir-free antimonate. This low-temperature enhancement may be due to the presence of some (25%) dimers with the composition Ir_2O_9 , and the consequent occurrence of short-range magnetic order. The data on the Sb-containing compounds are thus consistent with the proposal that the incompletely filled d-shell on the Ir cations plays an important role in the magnetic superexchange interactions. The distortion of the Ir site to a non-cubic symmetry ($3m$) could render the ground state magnetic, and a small magnetic moment would be introduced by population of the first excited electronic state. The susceptibility behaviour of $6\text{H Ba}_3\text{MgIr}_2\text{O}_9$ [17] suggests that the induced moment is small but finite, and we assume that it must be large enough to enhance the magnetic superexchange to a level significantly greater than that present in the Sb analogue.

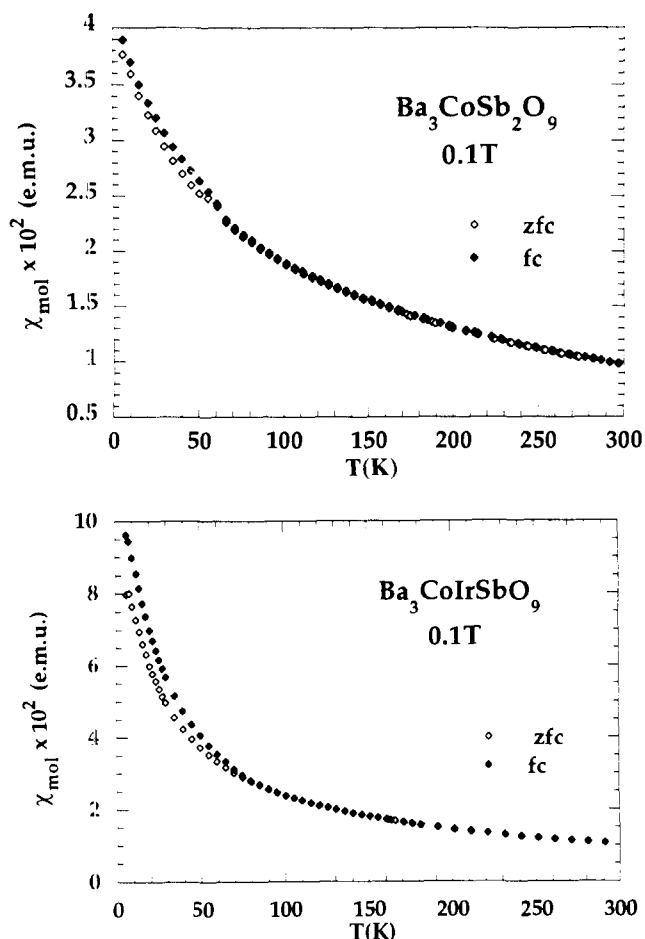


Fig. 6. The temperature dependence of the molar magnetic susceptibility of $\text{Ba}_3\text{CoSb}_2\text{O}_9$ and $\text{Ba}_3\text{CoIrSbO}_9$.

The occurrence of weak ferromagnetism appears [3] to be much more common in mixed metal oxides of Ir than in those of Ru. We believe that this is because the anisotropic superexchange interactions [18] which cause spin-canting are enhanced by the strong spin-orbit coupling found in elements from the third transition series. The observed temperature dependence of the magnetic susceptibility just below the Curie point might be due a variation in the spin-canting angle, but we believe it is more likely to be due to changes in the domain structure within our strongly magnetic sample. The compositions in the series $\text{Ba}_3\text{CoIr}_x\text{Ru}_{2-x}\text{O}_9$ having $x=1.85, 1.5, 1.0$ and 0.5 can all be considered as intermediate in behaviour between the two end members, $x=2.0$ and $x=0.0$. They each show weak ferromagnetism below a transition temperature which varies only slightly with composition, and the magnitude of the saturated magnetic moment decreases as the composition approaches that of the antiferromagnetic Ru end member ($x=0.0$). The behaviour of $\text{Ba}_3\text{CoIr}_{0.25}\text{Ru}_{1.75}\text{O}_9$ is very different in that the ZFC and FC susceptibilities diverge at a temperature ≈ 100 K above that of the susceptibility maximum, which is itself rather broad. The observation of magnetic hysteresis, perhaps

the consequence of spin blocking [19], at a temperature of ≈ 200 K is unlikely, in the light of our other data, to be due to the Co cations. It is more likely to arise as a consequence of coupling within the dimers. An isolated IrRuO_6 dimer would be ferrimagnetic rather than antiferromagnetic, and we tentatively suggest that at low Ir concentrations such magnetic dimers exist and give rise to the observed behaviour. At higher concentrations the number of IrRuO_6 groups will certainly increase, but so will spin-spin relaxation effects, resulting in a lack of hysteresis above the Neel temperature. A more careful examination of our data suggests that the susceptibility behaviour observed in $\text{Ba}_3\text{CoIr}_{0.25}\text{Ru}_{1.75}\text{O}_9$ persists, in a less marked way, in $\text{Ba}_3\text{CoIr}_{0.5}\text{Ru}_{1.5}\text{O}_9$, where there is a temperature interval of ≈ 18 K between the onset of hysteresis and the susceptibility maximum.

Further experimental work will be needed before the behaviour of these compounds is fully understood. The fact that we were able to achieve a satisfactory structure refinement for the Sb compound but not for the Ir/Ru compounds suggests that the latter may have a defect structure that merits investigation by electron microscopy. The above discussion assumes that Ir(V) and Co(II) are the only cation species present, and takes no account of the role of the small concentrations of Ir(IV) which would be formed if the anion sublattice were not fully occupied. The assumption concerning the nature of the dominant oxidation states in $\text{Ba}_3\text{CoIr}_x\text{Ru}_{2-x}\text{O}_9$ is based on the clear evidence of the bond lengths in BaLaCoIrO_6 and the ensuing generalization that Co(II)/Ir(V) is more stable in perovskite oxides than Co(III)/Ir(IV). However, it is worth noting that, following vibrational spectroscopy experiments, Treiber et al. [15] were uncertain about the assignment of oxidation states in the hexagonal compound. X-ray absorption spectroscopy or a neutron diffraction experiment could confirm our assumption. It would also be interesting to study $\text{Ba}_3\text{CoIr}_x\text{Ru}_{2-x}\text{O}_9$ in a low-temperature neutron diffraction experiment in order to ascertain whether the distortion to orthorhombic symmetry that was observed in the Ru end-member [8] occurs throughout the series, and also how the details of the magnetic structure vary with composition. However, the high absorption cross-section of Ir renders such experiments costly in terms of neutron beam time. Finally, we would like to understand why $\text{Ba}_3\text{NiIr}_2\text{O}_9$ does not [17] show magnetic behaviour akin to that of $\text{Ba}_3\text{CoIr}_2\text{O}_9$, even though BaLaCoIrO_6 and BaLaNiIrO_6 [3] have similar properties. The relatively large orbital contribution to the magnetic moment of Co^{2+} may take on a greater significance in the less isotropic hexagonal structure.

In conclusion, we have demonstrated that whereas Ir(V) can often be regarded as a non-magnetic cation when in a pseudo-cubic environment (BaLaCoIrO_6),

the magnetic moment induced by the population of an excited state or by the lowering of the site symmetry cannot always be ignored, as has been shown by a comparison of the behaviour of $\text{Ba}_3\text{CoIr}_2\text{O}_9$ with that of $\text{Ba}_3\text{CoSb}_2\text{O}_9$. The magnetic coupling through the Ir_2O_9 group in the former compound is also very different from that through the Ru_2O_9 group in the Ru analogue, $\text{Ba}_3\text{CoIr}_2\text{O}_9$ being a weak ferromagnet whereas $\text{Ba}_3\text{CoRu}_2\text{O}_9$ is an antiferromagnet.

Acknowledgements

We are grateful to the SERC for providing a contribution towards the cost of the SQUID magnetometer, a postgraduate studentship for JGG and access to neutron beam facilities. We thank R. Smith and S. Hull for their assistance with the neutron diffraction experiments.

References

- [1] F.J.J. Dijkema, J.F. Vente, E. Frikkee and D.J.W. Ijdo, *Mater. Res. Bull.*, 28 (1993) 1145.
- [2] J.B. Wiley and K.R. Poeppelmeier, *Mater. Res. Bull.*, 26 (1991) 1201.
- [3] A.V. Powell, J.G. Gore and P.D. Battle, *J. Alloys Comp.*, 201 (1993) 73.
- [4] K. Hayashi, G. Demazeau, M. Pouchard and P. Hagenmuller, *Mater. Res. Bull.*, 15 (1980) 461.
- [5] M. Walewski, B. Buffat, G. Demazeau, F. Wagner, M. Pouchard and P. Hagenmuller, *Mater. Res. Bull.*, 18 (1983) 881.
- [6] D. Jung, P. Gravereau and G. Demazeau, *Eur. J. Solid State Inorg. Chem.*, 30 (1993) 1025.
- [7] S.H. Kim and P.D. Battle, *J. Solid State Chem.*, in press.
- [8] P. Lightfoot and P.D. Battle, *J. Solid State Chem.*, 89 (1990) 174.
- [9] A.C. Larson and R.B. Von Dreele, General Structure Analysis System, *Los Alamos National Laboratory Report*, LAUR 86-748, 1990.
- [10] S. Hull and J. Mayers, *Rutherford-Appleton Laboratory Report*, RAL-89-118, 1989.
- [11] D.C. Khan and R.A. Erickson, *Phys. Rev. B*, 1 (1970) 2243.
- [12] G. Blasse, *J. Inorg. Nucl. Chem.*, 27 (1965) 993.
- [13] J.B. Goodenough, *Phys. Rev.*, 171 (1968) 466.
- [14] P.D. Battle and W.J. Macklin, *J. Solid State Chem.*, 52 (1984) 138.
- [15] U. Treiber, S. Kemmler-Sack and A. Ehmann, *Z. Anorg. Allg. Chem.*, 487 (1982) 189.
- [16] J. Darriet, M. Drillon, G. Villeneuve and P. Hagenmuller, *J. Solid State Chem.*, 19 (1976) 213.
- [17] R.C. Byrne and C.W. Moeller, *J. Solid State Chem.*, 2 (1970) 228.
- [18] T. Moriya, *Phys. Rev.*, 120 (1960) 91.
- [19] A. Labarta, R. Rodriguez, L. Balcells, J. Tejada, X. Obradors and F.J. Berry, *Phys. Rev. B*, 44 (1991) 691.